

Carbogen Breathing Differentially Enhances Blood Plasma Volume and 5-Fluorouracil Uptake in Two Murine Colon Tumor Models with a Distinct Vascular Structure¹

Hanneke W. M. van Laarhoven*, Giulio Gambarota[†], Jasper Lok[‡], Martin Lammens[§], Yvonne L. M. Kamm*, Theo Wagener*, Cornelis J. A. Punt*, Albert J. van der Kogel[‡] and Arend Heerschap[†]

Departments of *Medical Oncology, [†]Radiology, [‡]Radiation Oncology, and [§]Pathology, Radboud University Nijmegen Medical Centre, Nijmegen, The Netherlands

Abstract

For the systemic treatment of colorectal cancer, 5-fluorouracil (FU)-based chemotherapy is the standard. However, only a subset of patients responds to chemotherapy. Breathing of carbogen (95% O₂ and 5% CO₂) may increase the uptake of FU through changes in tumor physiology. This study aims to monitor in animal models *in vivo* the effects of carbogen breathing on tumor blood plasma volume, pH, and energy status, and on FU uptake and metabolism in two colon tumor models C38 and C26a, which differ in their vascular structure and hypoxic status. Phosphorus-31 magnetic resonance spectroscopy (MRS) was used to assess tumor pH and energy status, and fluorine-19 MRS was used to follow FU uptake and metabolism. Advanced magnetic resonance imaging methods using ultra-small particles of iron oxide were performed to assess blood plasma volume. The results showed that carbogen breathing significantly decreased extracellular pH and increased tumor blood plasma volume and FU uptake in tumors. These effects were most significant in the C38 tumor line, which has the largest relative vascular area. In the C26a tumor line, carbogen breathing increased tumor growth delay by FU. In this study, carbogen breathing also enhanced systemic toxicity by FU.

Neoplasia (2006) 8, 477–487

Keywords: Carbogen, colon carcinoma, 5-fluorouracil, ¹⁹F MRS, ³¹P MRS.

A critical factor in the success of the systemic treatment of advanced colorectal cancer may be adequate drug delivery by the vascular network to metastases. Tumor hypoxia, which results from poor vascularization or which may even be a constitutive characteristic of solid tumors [2,3], contributes to drug resistance [4]. Recently, it was demonstrated that a substantial amount of hypoxia is present in liver metastases of patients with colorectal cancer [5].

Breathing carbogen, a gas mixture of 95% O₂ and 5% CO₂, has been shown to increase the uptake of anticancer drugs, such as ifosfamide [6,7] and FU [8–10], in rodent solid tumors. Carbogen breathing may induce several physiological changes—a decrease in tumor hypoxia, an increase in tumor blood flow, a decrease in extracellular pH (pH_e), and an increase in tumor energy status—which may all contribute to an improved uptake of chemotherapeutic drugs. However, these physiological changes do not occur in all experimental tumor lines [11], and response to carbogen breathing may be heterogeneous within a tumor [12]. In addition, it has been hypothesized that an increase in tumor blood flow may, in itself, be insufficient for an increased uptake of FU in solid tumors because not only drug delivery but also drug clearance will be increased [10]. Therefore, for carbogen to increase FU uptake, a secondary mechanism, apart from an increase in tumor blood flow, may be necessary.

The murine colon carcinoma lines C38 and C26a are known as well-differentiated and poorly differentiated colon carcinoma [13], respectively, with a differently structured vascular network and different patterns of hypoxia, as is illustrated in Figure 1 [14]. In previous experiments, the tumor doubling time of

Introduction

Colorectal cancer is one of the most frequently occurring cancers in the western world. For almost two decades, 5-fluorouracil (FU), in combination with leucovorin, has been regarded as the standard adjuvant and palliative treatment of primary colon cancer and advanced colorectal cancer, respectively. FU is used as a radiosensitizer, in combination with radiation therapy, of rectal cancer. Although new classes of drugs have become available, FU and other fluoropyrimidines remain part of the treatment of colorectal cancer [1].

Abbreviations: 3-APP, 3-aminopropylphosphonate; FBAL, α -fluoro- β -alanine; FU, 5-fluorouracil; FUPA, α -fluoro- β -ureidopropionic acid; MRS, magnetic resonance spectroscopy; β NTP, β -nucleoside triphosphate; USPIO, ultrasmall superparamagnetic particles of iron oxide; Pcr, phosphocreatine; Pi, inorganic phosphate

Address all correspondence to: Hanneke W. M. van Laarhoven, Department of Medical Oncology 452, Radboud University Nijmegen Medical Centre, PO Box 9101, 6500 HB Nijmegen, The Netherlands. E-mail: h.vanlaarhoven@onco.umcn.nl

¹This study was financially supported by the Dutch Cancer Society (grant KUN 2000-2307). Received 11 January 2006; Revised 8 March 2006; Accepted 8 March 2006.

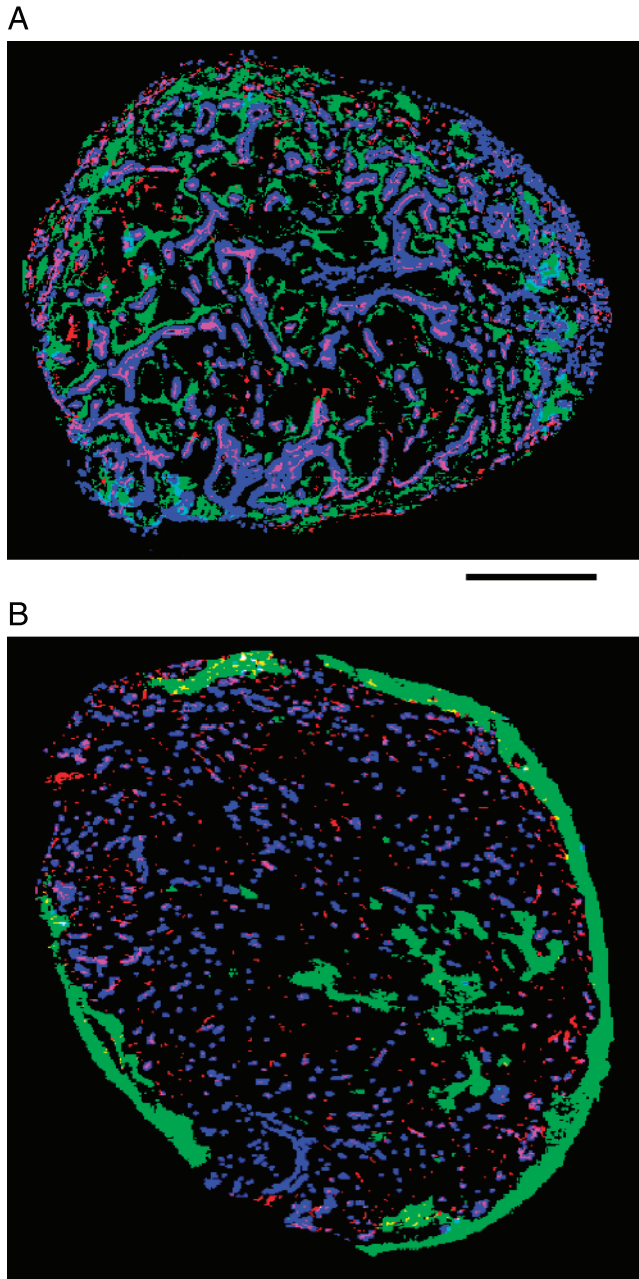


Figure 1. Binary image of complete tumor sections of C38 (A) and C26a (B) colon tumors showing the pattern of vascular architecture (stained with 9F1, which is a rat monoclonal to the mouse endothelium), perfused vessels (Hoechst33342 staining), and hypoxic profile (pimonidazole staining). Vascular structures, red–pink; perfused vessels, blue; hypoxic areas, green. The solid line indicates 1 mm. For further details on the immunohistochemical methods used, refer to Van Laarhoven et al. [14].

untreated C26a tumors was 3 days, whereas the tumor doubling time of untreated C38 tumors was 4.9 days [13]. C26a tumors are less responsive to FU than are C38 tumors [13]. Previously, it has been shown that both C38 and C26a tumors respond to carbogen breathing by a decrease in tumor hypoxia [14]. Changes in other key physiological parameters caused by carbogen breathing, which may alter FU response, have neither been studied in these models nor

in other colon tumor models. Therefore, the aim of this study was to monitor the effect of carbogen breathing on tumor blood plasma volume, pH, and energy status, and on FU uptake and metabolism in C38 and C26a colon tumors. Because these effects are monitored best *in vivo*, phosphorus-31 magnetic resonance spectroscopy (MRS) was used to assess tumor pH and energy status [15], and fluorine-19 (^{19}F) MRS was used to follow FU uptake and metabolism [16]. Advanced magnetic resonance imaging (MRI) methods using ultrasmall superparamagnetic particles of iron oxide (USPIO) were applied to study blood plasma volume [17]. The results showed that, by an increase in tumor blood plasma volume, carbogen breathing can significantly increase FU uptake and efficacy in murine colon tumors.

Materials and Methods

Tumors

The C38 and C26a murine colon tumors were acquired from Dr. G. J. Peters of the Vrije Universiteit (Amsterdam, The Netherlands). Viable C38 and C26a tumor tissue fragments with a diameter of 1 to 3 mm were implanted subcutaneously in the right flank of C57BL/6 and Balb/C mice, respectively. Animals were kept according to institutional guidelines for animal care. For MRS experiments, the mean tumor volume \pm standard error of the mean (SEM) calculated from length \times width \times height \times $\pi/6$ (mm^3) was 362.2 ± 60.8 for C26a control tumors, 478.0 ± 66.5 for C26a carbogen-treated tumors, 243.5 ± 24.4 for C38 control tumors, and 224.6 ± 49.8 for C38 carbogen-treated tumors. These tumor volumes were not significantly different from each other, except for the C26a carbogen-treated tumors, which had a significantly larger tumor volume than the C38 carbogen-treated tumors. However, no direct comparisons of MRS data were made between C26a carbogen-treated tumors and C38 carbogen-treated tumors. For MRI experiments, the mean tumor volume \pm SEM (mm^3) was 354.8 ± 97.1 for control tumors, 320.1 ± 39.6 for C26a carbogen-treated tumors, and 253.9 ± 23.3 for C38 carbogen-treated tumors. These tumor volumes were not significantly different from each other. For growth experiments, the mean tumor volume \pm SEM (mm^3) was 86.6 ± 11.2 for C26a control tumors, 101.5 ± 11.7 for C26a carbogen-treated tumors, 100.7 ± 10.5 for C38 control tumors, and 80.6 ± 4.3 for C38 carbogen-treated tumors. These tumor volumes were not significantly different from each other. All experiments were approved by the institutional ethical committee for animal use.

Hardware for MR Examinations

All MR experiments were performed on an SMIS 7-T horizontal bore animal system. A homemade $^{31}\text{P}/^{19}\text{F}$ double-tuned 10-mm surface radiofrequency (RF) coil that was also tunable to ^1H was used as a transmitter/receiver [18]. After mice had been anesthetized with isoflurane (1.5–2%), oxygen (30%), and nitrous oxide (68%), the tumor was positioned at the center of the coil. During measurements, body temperature was monitored with a rectal fluoroptic probe (Luxtron 712;

Luxtron Corporation, Santa Clara, CA) and maintained at constant body temperature with a warm water pad.

$^{31}\text{P}/^{19}\text{F}$ MR Measurements

A nonlocalized $^{31}\text{P}/^{19}\text{F}$ interleaved pulse-acquire sequence with a 90° rectangular RF pulse of 20 microseconds was used in all experiments. Each ^{31}P scan was alternated with six ^{19}F scans. The repetition time (T_R) for ^{31}P MR acquisition was 3 seconds; for ^{19}F , $T_R = 430$ milliseconds, with a total measurement time of 4 minutes. In total, 31 sequential measurements were performed.

As a marker of pH_e , 3-aminopropylphosphonate (3-APP; Sigma-Aldrich, Zwijndrecht, The Netherlands) was injected intraperitoneally through a catheter approximately 10 minutes before the start of carbogen breathing (Figure 2A). In 10 mice with a C38 tumor and in 12 mice with a C26a tumor, the breathing gas was switched to carbogen 5 minutes before the start of $^{31}\text{P}/^{19}\text{F}$ MRS measurements and was continued with carbogen for 28 minutes (i.e., during the first seven measurements). Then FU (Teva, Mijdrecht, The Netherlands) was administered (150 mg/kg) intraperitoneally within 10 seconds before start of the first $^{31}\text{P}/^{19}\text{F}$ MRS measurement. Twelve mice with a C38 tumor and 10 mice with a C26a tumor did not undergo carbogen breathing and served as controls.

MR data were processed using jMRUI, version 2.0 (<http://www.mrui.uab.es/mrui/mruiHomePage.html>). Intracellular pH (pH_i) and pH_e were calculated using the chemical shift difference between inorganic phosphate (Pi) and phosphocreatine (PCr), and between 3-APP and PCr, respectively

[19]. The energy status of the tumor at each time point was represented by the ratio of β -nucleoside triphosphate (βNTP) to Pi ($\beta\text{NTP}/\text{Pi}$). Using Graphpad Prism, GraphPad Software, Inc., San Diego, CA (version 4), quantitative changes in the integrals of FU resonances were fitted to a biexponential equation for each mouse, according to: $Y = C_{\text{FU}}[1 - \exp(-0.693x/t_{\text{uptake}})]\exp[-0.693x/t_{1/2}]$, where C_{FU} refers to the maximum concentration (a.u.) of FU, t_{uptake} refers to the time (minutes) up to 50% of the maximum FU resonance amplitude in the tumor, $t_{1/2}$ refers to the half-life (minutes) of FU in the tumor, and x refers to the measurement of time (minutes). If the data fitting this equation would not converge, a monoexponential equation is used, according to: $Y = C\exp(-0.693x/t_{1/2})$. Quantitative changes in the resonances of anabolites, which are active metabolites of FU, and of catabolites α -fluoro- β -ureidopropionic acid (FUPA) and α -fluoro- β -alanine (FBAL), were fitted to a monoexponential equation, according to: $Y = C_{\text{anab,FUPA,FBAL}}\{1 - \exp[-(0.693/t_{\text{uptake}})(x - B)]\}$, in which $C_{\text{anab,FUPA,FBAL}}$ refers to the maximum concentration (a.u.) of the anabolite FUPA or FBAL, and B refers to the time interval (minutes) between the start of the measurement and the appearance of the resonances of the anabolite FUPA or FBAL. The ^{19}F MRS data of individual mice were included for further calculations and comparisons to determine if $R^2 \geq 0.8$.

MRI Measurements

As a measure of relative blood plasma volume, quantitative measurements of changes in the T_1 relaxation rate of

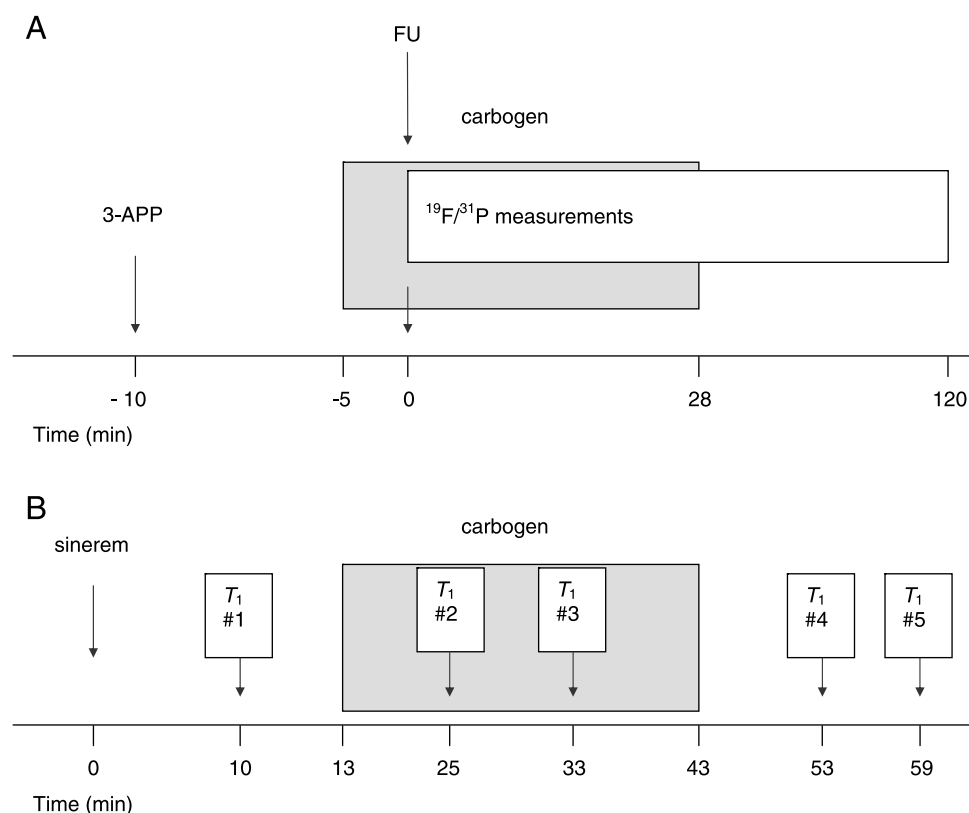


Figure 2. Experimental design of MRS (A) and MRI (B) experiments (for details, see the Materials and Methods section).

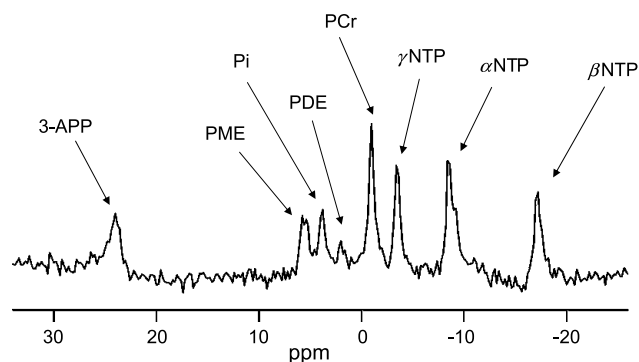


Figure 3. ^{31}P MR spectrum of a C26a tumor. Resonances of 3-APP as a marker of pH_e , phosphomonoesters (PME), Pi, phosphodiester (PDE), PCr, and high-energy phosphates (NTP) are shown. The acquisition started 12 minutes after FU injection. No carbogen breathing was applied.

water proton spins were used after the administration of a contrast agent consisting of USPIO [17,20].

After three gradient-echo scout MR images for anatomic localization of the tumor, high-resolution multislice gradient-echo images were acquired to identify one slice of interest through the center of the tumor. Inversion recovery snapshot fast low-angle shot was performed to measure water T_1 relaxation time [image matrix size = 64×64 ; field of view = 3×3 cm; slice thickness (SLT) = 1.6 mm; T_R = 5 milliseconds; echo time (T_E) = 2.7 milliseconds; inversion time (T_I) = $52 + n \cdot 320$ milliseconds, where $n = 0, 1, 2, \dots, 15$]. T_1 relaxation times were measured at 1 hour after USPIO administration at five time points (Figure 2B). The USPIO blood pool contrast agent sinerem ($150 \mu\text{mol/kg Fe}$; Guerbet, Roissy CDG Cedex, France) was injected intravenously through a catheter inserted into the tail vein of all mice. In six mice with a C38 tumor and in six mice with a C26a tumor, carbogen breathing was started 13 minutes after the injection of sinerem (injected for 30 minutes). Three mice with a C38 tumor and four mice with a C26a tumor did not undergo carbogen breathing and served as controls.

The Levenberg Marquardt nonlinear least squares algorithm was used to analyze T_1 data. The algorithm was implemented with MatLab (Mathworks, Natick, MA). For each tumor, voxel-by-voxel maps of apparent T_1 (T_1^*) were generated from a three-parameter fit of image intensities according to the equation: $S = A + B \exp(-nT_1/T_1^*)$. The value of the corrected T_1 was calculated from the formula: $T_1 = T_1^* (B/A - 1)$. For each tumor, R_1 ($R_1 = 1/T_1$) maps were obtained at all time points. From each map, the mean R_1 was calculated by drawing a region of interest, which included the whole tumor, on the R_1 map and by averaging the values of all pixels. The values of the mean R_1 at all time points were normalized to the value of the first time point. The mean R_1 relaxation rate in controls was then compared with the mean R_1 in treated tumors, at each time point.

Tumor Growth and FU Toxicity

Separate groups of mice were followed for tumor volume for 20 days after treatment with FU as a single treatment or in

combination with carbogen breathing, using caliper measurements (control C38, $n = 7$; control C26, $n = 8$; carbogen C38, $n = 7$; carbogen C26a, $n = 8$). To each group, four to five mice were added to monitor systemic toxicity only. Carbogen breathing was started 5 minutes before the intraperitoneal administration of FU (150 mg/kg) and continued for 25 minutes after FU injection. Because several mice that underwent carbogen breathing were found to be severely ill after approximately 10 days, pathological analysis was performed on paraffin-embedded biopsies of the heart, lungs, intestines, muscles, kidneys, spleen, pancreas, and long bones, using hematoxylin and eosin staining of the material.

Results

^{31}P MRS Measurements

To monitor changes in pH and energy status during and after carbogen breathing, ^{31}P MRS was performed on C38 and C26a tumors. A typical ^{31}P MR spectrum from a C26a tumor is shown in Figure 3. pH_i and pH_e were calculated from the chemical shift difference between the resonances of Pi and PCr, and between 3-APP and PCr, respectively. The energy status of the tumors was assessed by $\beta\text{NTP}/\text{Pi}$. Table 1 summarizes the mean values of pH and the energy status throughout measurements in the control groups of C38 and C26a tumors. Higher pH_i and pH_e were found in C38 tumors compared to C26a, but a lower ΔpH ($\Delta\text{pH} = \text{pH}_e - \text{pH}_i$) was found. In both tumor lines, ΔpH was positive. The $\beta\text{NTP}/\text{Pi}$ energy status of C38 tumors was more than one and a half times higher than that of C26a tumors.

The pH and energy status of C38 and C26a tumors 2 hours after the injection of FU as a single treatment or in combination with carbogen breathing are shown in Figure 4. In both C38 and C26a tumors, pH_i remained constant throughout the measurement. In contrast, pH_e decreased significantly in C38 tumors 15 minutes after the start of carbogen breathing, compared with the control group, and remained significantly lower for 32 minutes. In C26a tumors, a similar but less pronounced pattern was observed. In C38 tumors, the decrease in pH_e was large enough to result in a decrease in ΔpH . The energy status of both tumor lines, as assessed from the $\beta\text{NTP}/\text{Pi}$ ratio, remained constant throughout the experiment.

^{19}F MRS Measurements

^{19}F MRS was used to monitor the uptake and metabolism of FU in C38 and C26a tumors. Figure 5 shows a typical ^{19}F

Table 1. pH and Energy Status of C38 and C26a Tumors.

	pH_i	pH_e	ΔpH	$\beta\text{NTP}/\text{Pi}$
C38	$7.05 \pm 0.00^*$	$7.22 \pm 0.00^*$	$0.18 \pm 0.00^*$	$2.20 \pm 0.02^*$
C26a	6.89 ± 0.00	7.11 ± 0.00	0.22 ± 0.00	1.33 ± 0.02

Mean pH and energy status \pm SEM are shown for C38 and C26a tumors from the control groups.

*Indicates statistically significant differences between C38 and C26a tumors ($P < .001$).

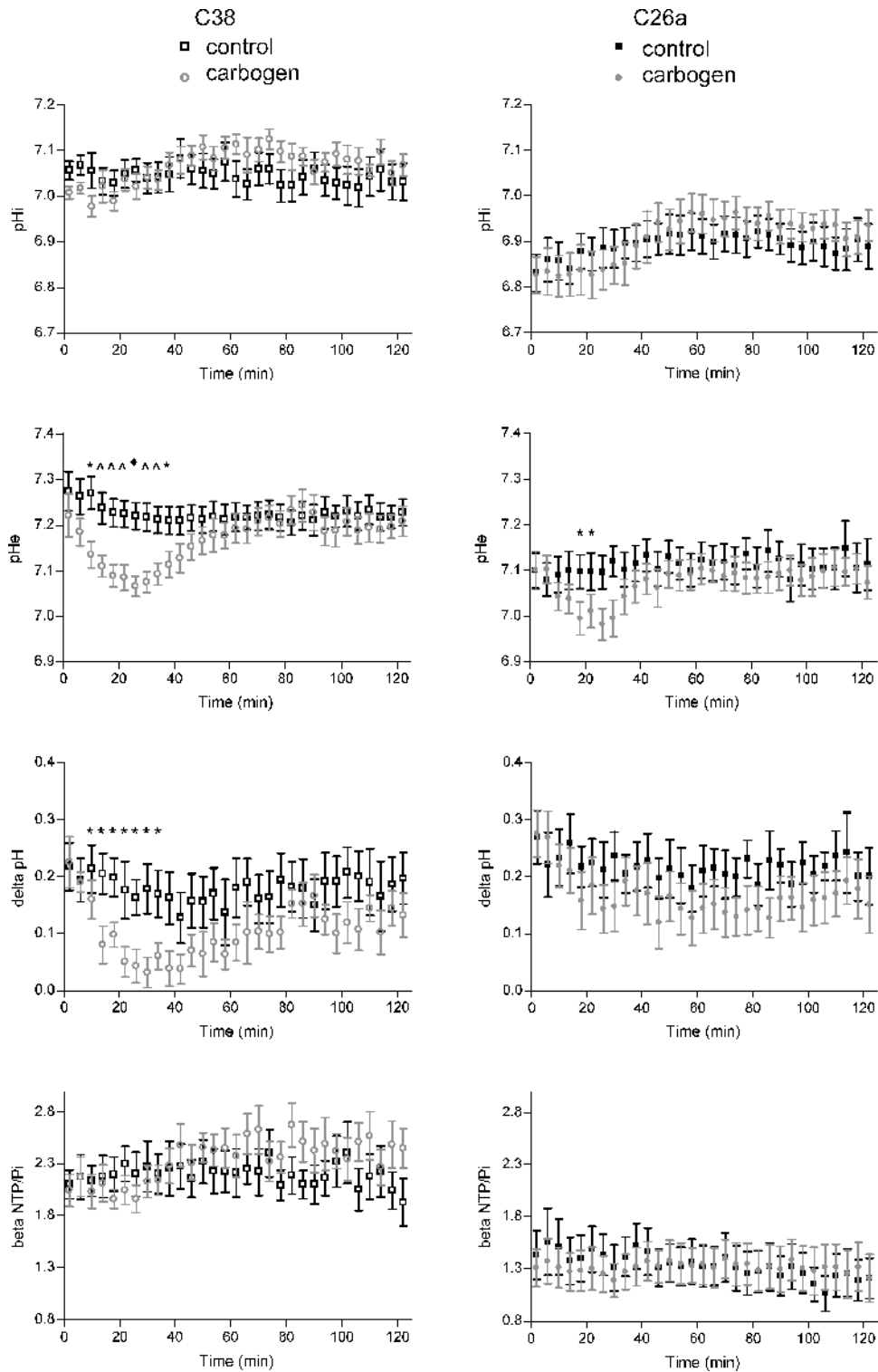


Figure 4. pH_i , pH_e , ΔpH ($pH_e - pH_i$), and energy status ($\beta NTP/\beta i$) for C38 (left) and C26a (right) tumors of the control group and of the carbogen breathing group. The error bar indicates SEM. A significant difference between the control group and the carbogen breathing group is indicated by * $P < .05$; ^ $P < 01$; ♦ $P < .001$. Carbogen breathing is started at $t = -5$ minutes and is terminated at $t = 28$ minutes; FU is injected at $t = 0$.

MR spectrum from a C26a tumor. In most of the tumors, not only resonance of FU but also resonances of anabolites and of the catabolite FUPA were detected. Resonance of FBAL was present in a minority of tumors. Due to movement artifacts in two tumors from the C26a groups, two tumors

from the C38 control group, and one tumor from the C38 carbogen breathing group, changes in ^{19}F MR resonance integrals could not be fitted to a monoexponential equation or to a biexponential equation with an $R^2 \geq 0.80$. The data of these tumors were excluded from analysis. Because the

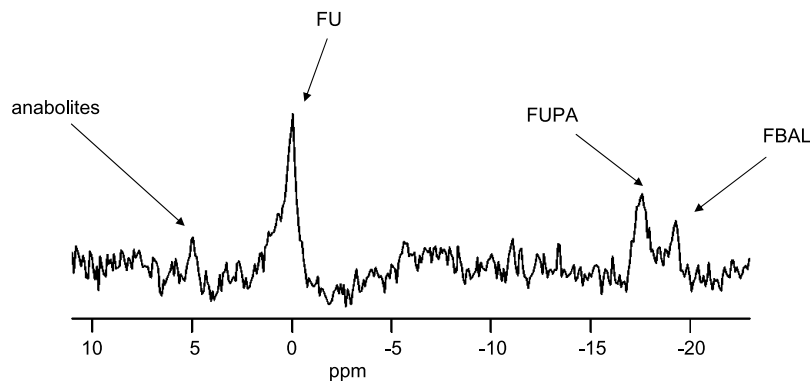


Figure 5. ^{19}F MR spectrum of a C26a tumor. Resonances of anabolites, FU, and the catabolites FUPA and FBAL are shown. The acquisition of this spectrum started 60 minutes after FU injection at $t = 0$. Carbogen breathing was applied from $t = -5$ minutes to $t = 28$ minutes.

signal-to-noise ratio of the resonances of anabolites and of the catabolite FBAL was too low to provide an adequate fit to a monoexponential equation or to a biexponential equation in most mice, further analyses on the pharmacokinetics of FU and FUPA were performed.

C38 tumors had a significantly larger amount of FU and a faster uptake of FU compared to C26a tumors (Table 2). The half-life of FU in C38 tumors was significantly longer than in C26a tumors, and the total amount of FU that was present in C38 tumors (as measured by the average resonance integral of FU) was higher. After carbogen breathing, C_{FU} increased in both tumor lines, but the increase was significant for C38 tumors only. In both tumor lines, t_{uptake} decreased (i.e., FU was taken up faster), which was significant for C26a tumors. In both tumor lines, the average of all measured resonance integrals in time increased on carbogen breathing, which was significant for C38 tumors. The appearance of FUPA in C38 and C26a tumors was also monitored. In C38 tumors, the resonance integral of FUPA increased throughout the measurement period, whereas in C26a tumors, a plateau was reached. The average of all measured resonance integrals in time of FUPA was significantly higher in C38 tumors (Table 3). However, the average resonance integral of FUPA in C38 tumors divided by the average resonance integral of FU was significantly lower than that in C26a tumors. After

carbogen breathing, the average resonance integral of FUPA divided by the average resonance integral of FU significantly decreased in C38 tumors compared with control tumors.

MRI Measurements

To assess the changes in blood plasma volume, the relaxation rate R_1 was determined for each tumor at five different time points. In Figure 6, the fractional change in the relaxation rate R_1 is shown before, during, and after carbogen breathing for the C38 and C26a tumors. In both tumor lines, a significant increase in R_1 was observed during carbogen breathing, which corresponds to an increase in tumor blood plasma volume. The fractional increase in relative tumor blood plasma volume during carbogen breathing was larger in C38 tumors than in C26a tumors, which was statistically significant when taking the two time points during carbogen breathing together ($P = .03$). After terminating carbogen breathing, R_1 quickly returned to control values in C38 tumors, whereas R_1 remained significantly higher in C26a tumors than in the control group.

Tumor Growth and FU Toxicity

To determine whether carbogen breathing increased FU efficacy, the growth of C38 and C26a tumors was measured after the administration of FU as a single agent or in

Table 2. Pharmacokinetics of FU in C38 and C26a Tumors.

	C_{FU} (a.u.)	t_{uptake} (min)	$t_{1/2}$ (min)	Average of All Measured FU Resonance Integrals in Time (a.u.)
C38 control ($n = 10$)	1603 \pm 96.9*	0.94 \pm 0.35 [†]	72.99 \pm 8.69 [‡]	929.0 \pm 55.3 [§]
C38 carbogen ($n = 9$)	2223 \pm 85.5 [¶]	0.71 \pm 0.20	65.16 \pm 4.63	1223 \pm 82.2 [#]
C26a control ($n = 7$)	581.2 \pm 37.6	2.30 \pm 0.48	33.17 \pm 2.56	192.9 \pm 23.6
C26a carbogen ($n = 10$)	665.3 \pm 31.3	0.54 \pm 0.22**	33.00 \pm 2.12	231.6 \pm 31.2

The mean of the maximum concentration of FU (C_{FU}), the doubling time of FU resonance integral increase in the tumor (t_{uptake}), the half-life of FU in the tumor ($t_{1/2}$), and the average of all resonance integrals (average FU resonance integral) \pm SEM are shown for C38 and C26a tumors. Values are calculated from a fit of the mean resonance integral of all mice per group to a biexponential equation (see the Materials and Methods section).

* $P < .0001$, compared with the C26a control group.

[†] $P < .05$, compared with the C26a control group.

[‡] $P < .01$, compared with the C26a control group.

[§] $P < .0001$, compared with the C26a control group.

[¶] $P < .001$, compared with the C38 control group.

[#] $P < .001$, compared with the C38 control group.

** $P < .01$, compared with the C26a control group.

Table 3. Uptake of FUPA in C38 and C26a Tumors.

	Mean of All Measured FUPA Resonance Integrals in Time (a.u.)	Mean of the Total FUPA Resonance Amplitude Divided by the Total FU Resonance Amplitude
C38 control (n = 5)	306.2 ± 36.0*	1.1 ± 0.2 [†]
C38 carbogen (n = 5)	278.2 ± 33.8	0.3 ± 0.1 [‡]
C26a control (n = 4)	154.6 ± 16.7	3.3 ± 0.8
C26a carbogen (n = 8)	144.2 ± 14.9	3.1 ± 0.9

The mean of the total FUPA resonance amplitude and the mean of the total FUPA resonance amplitude divided by the total FU resonance amplitude ± SEM are shown for C38 and C26a tumors.

*P < .001, compared with the C26a control group.

[†]P < .05, compared with the C26a control group.

[‡]P < .0001, compared with the C38 carbogen group.

combination with carbogen breathing. In C26a tumors, carbogen breathing increased FU efficacy, as is shown in Figure 7.

Approximately 10 days after the start of treatment, we observed that, compared with the mice receiving FU only, more mice in the groups that received FU combined with carbogen breathing died or were severely ill (as indicated by hair loss, shivering, and loss of mobility), and the mice were sacrificed because of bioethical reasons. Mortality at 13 days was significantly higher after carbogen breathing combined with FU, compared to FU only. Pathological analysis of the biopsies of heart muscles of ill mice showed increased hypercontraction and eosinophilia of muscle fibers indicative of acute ischemic infarction. In the bone marrow of the long bones of diseased mice, a marked increase in megakaryocytes, which were also considerably variable in size, was observed, compared with healthy mice. This may be considered as a sign of thrombocytopenia. The lungs, intes-

tines, muscles, kidneys, spleen, and pancreas did not show abnormalities, except for pulmonary edema in one mouse.

Discussion

The key observation of this study was that carbogen breathing had significant but different effects on the physiology and FU uptake of two murine colon carcinoma lines. However, carbogen breathing also enhanced the systemic toxicity of FU.

A consistent effect of carbogen breathing on tumor physiology in different experimental tumor lines is a decrease in tumor hypoxia [10,11,14,21,22], although the magnitude of this effect varied in different tumor lines [12,23]. As tumor hypoxia may contribute to drug resistance [4], carbogen breathing could improve the efficacy of chemotherapy. The classic explanation for a decrease in tumor hypoxia by carbogen breathing is an increase in oxygen transport by blood plasma [24]. However, several other changes in tumor physiology have been described after carbogen breathing, such as changes in (blood) pH, energy status, and blood flow. These changes may not only have an impact on tumor hypoxia but also directly influence the uptake and metabolism of chemotherapeutic agents.

Changes in pH

In this study, a decrease in pHe due to carbogen breathing was observed in C38 and C26a tumors. A similar effect has been described in, for example, RIF-1 tumors [9], GH3 xenografts [10], and hepatomas [25]. In C38 tumors, the decrease in pHe resulted in a decrease in ΔpH. Previously, it has been shown that uptake of FU in isolated tumor cells may be pH-dependent [15,26]. In fact, in C38 tumors, we observed an increase in FU uptake (C_{FU}).

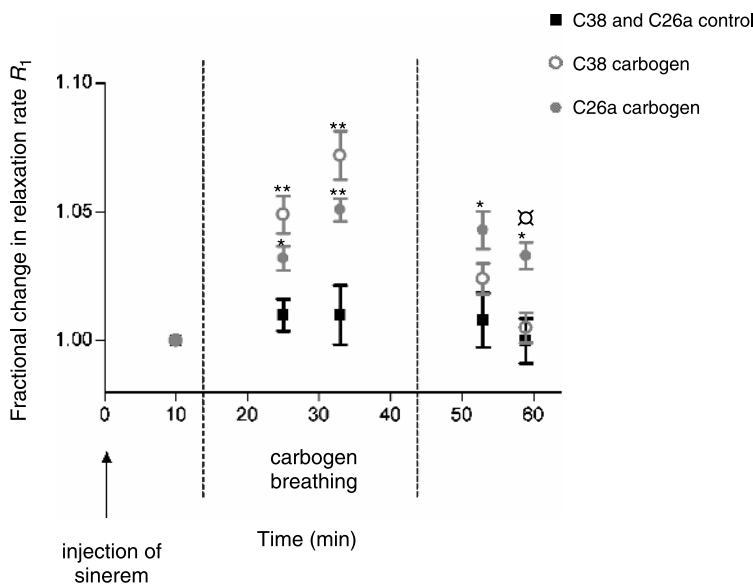


Figure 6. Fractional change in the longitudinal relaxation rate R_1 for C38 and C26a tumors 3 minutes before the start of carbogen breathing, during carbogen breathing, and after the termination of carbogen breathing. *Significant difference ($P < .05$) between the control group and the carbogen breathing group. **Significant difference ($P < .01$) between the control group and the carbogen breathing group. [□]Significant difference ($P < .01$) between C38 and C26a tumors. The error bars indicate SEM.

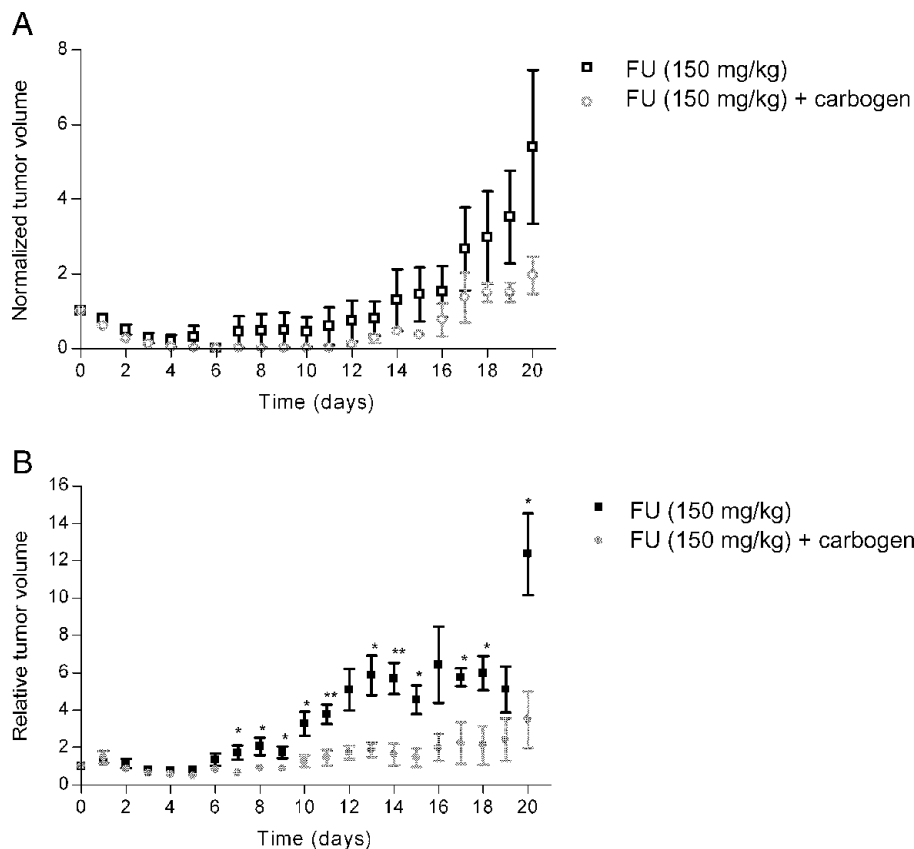


Figure 7. Growth curves of C38 (A) and C26a tumors (B) after the administration of FU (150 mg/kg) as a single treatment or in combination with carbogen breathing. Tumor volumes are normalized to 1 on day 0, which is the day of treatment. Error bars indicate SEM. *Significant difference ($P < .05$) between the control group and the carbogen breathing group. **Significant difference ($P < .01$) between the control group and the carbogen breathing group.

It should be noted that, for ^{31}P MRS measurements (and ^{19}F MRS measurements), a nonlocalized acquisition technique was used to obtain sufficient time resolution. This implies that some contributions (<30%) from muscles and the skin will be present.

Energy Status

The pretreatment energy status (NTP/Pi) of chemically induced primary rat mammary tumors has been shown to be a predictor of tumor response [27,28]. It has been hypothesized that an elevated energy status may reflect a well-vascularized tumor, which has more capacity for energy-dependent FU uptake and anabolism [27]. In this study, a large difference in energy status was observed between C38 and C26a tumors, with relatively high values for C38 tumors. Previously, it has been shown that the tumor energy status decreased when mean intercapillary distance increased (i.e., tumor perfusion decreased) [29]. As the C38 tumor is a well-perfused tumor [14], this could explain the relatively higher levels of NTP/Pi in C38 than in C26a tumors. The large difference in energy status between C38 and C26a tumors corresponds well to the difference in relative blood plasma volume [17] and relative vascular area [14] in these tumor lines, as well as to the difference in chemotherapy sensitivity [13].

In subcutaneous hepatomas, an increase in NTP/Pi was observed during carbogen breathing, whereas energy status in GH3 xenografts remained constant [10]. For human gliomas implanted subcutaneously in mice, a decrease in energy status on carbogen breathing has been observed [11], which was likely due to the so-called steal effect (as described by Jirtle [30]; see below). In subcutaneous C38 and C26a tumors, no difference in energy status between the control group and the carbogen breathing group was observed.

Blood Plasma Volume

In the slower-growing C38 tumors, compared to the faster-growing C26a tumors, a larger blood plasma volume [17] and a relative vascular area have been observed [14]. This could explain the higher maximum concentration of FU and the higher average resonance integral of FU and FUPA in C38 tumors. The higher maximum concentration and the average resonance integral of FU in C38 tumors, as well as the longer half-life of FU, may contribute to the higher chemosensitivity of C38 tumors compared to C26a tumors, which has been described before [13].

The effects of carbogen on the tumor vasculature are usually measured in terms of tumor blood flow and/or vascular diameter. O_2 has been shown to have a vasoconstrictive

effect on both immature and mature tumor vessels [31]. In theory, the CO₂ component of carbogen (95% O₂ and 5% CO₂) may overcome the vasoconstrictive effects of O₂. However, in this respect, variable effects of carbogen breathing have been reported. In subcutaneously or intramuscularly implanted R3230Ac tumors, carbogen had no consistent effect on tumor blood flow measured by Doppler flowmetry [23]. In another study with the same tumor model, carbogen breathing resulted in a transient reduction in tumor arteriolar diameter measured by intravital microscopy and a reduction in tumor blood flow measured by Doppler flowmetry [32]. In subcutaneous human glioblastomas, a decrease in tumor blood flow after carbogen breathing was observed by fast dynamic ¹H MRI of Gd-DTPA uptake [11], possibly due to a steal effect [30]. The steal effect refers to a situation wherein the tumor vasculature lacks a responsive smooth musculature and is in parallel with the host vasculature. Tumor blood perfusion could then be reduced during carbogen breathing due to a vasodilating effect of the CO₂ component of carbogen on host vessels. In this study, tumor blood plasma volume was assessed using MR methods, with ultrasmall superparamagnetic iron oxide as a contrast agent. In both C38 and C26a tumors, a significant increase was observed in the relaxation rate R_1 , which is proportional to an increase in relative tumor blood plasma volume. Therefore, these results suggest a vasodilating effect of carbogen breathing, rather than a vasoconstrictive or steal effect, in C38 and C26a tumors. This is the first study to show an increased relative tumor blood plasma volume after carbogen breathing using this MR approach. The advantage of this technique, in contrast with measurements of vascular diameter, is that it could be applied not only in subcutaneous (window chamber) models but also in orthotopic models. Moreover, the interpretation of data for this study is more straightforward than, for example, that for blood oxygenation-dependent MRI measurements, which reflect a combination of blood oxygenation, flow, and volume responses [33].

Because MRI techniques using blood pool agents measure the volume of plasma-perfused vessels and do not account for hematocrit (i.e., potential oxygen-carrying erythrocytes), they may overestimate oxygen delivery [33]. For the delivery of chemotherapy, plasma-perfused vascular volume rather than vascular volume occupied by erythrocytes is of primary importance, although tumor hypoxia may be related to chemotherapy resistance [34]. The observed increase in relative tumor blood plasma volume after carbogen breathing implies that the vascular surface area in the tumor is increased, which could lead to an improved tumor uptake of FU. In both C38 and C26a tumors, C_{FU} and the average of all measured FU resonance integrals in time were increased in the carbogen breathing group compared to those in the control group, although this was significant for C38 tumors only. In fact, blood plasma volume response to carbogen breathing was also larger in C38 tumors than in C26a tumors. Previously, similar ¹⁹F MRS results were reported for C38 tumors when carbogen breathing was initiated 1 minute before and maintained 8.5 minutes after FU (150 mg/kg) bolus injection [8]. In that study, increased levels of FU, as well as

increased levels of anabolites and catabolites, without enhanced FU retention in the tumor were found. In the present study, after terminating carbogen breathing, the relative blood plasma volume in C38 tumors returned to control values more quickly than the relative blood plasma volume in C26a tumors. This indicates a difference in responsive tumor vasculature in C38 and C26a tumors. In fact, on a microscopic level, the tumor vasculature of C38 and C26a tumors is rather different: C38 tumors mainly show large vessels in a corded structure, whereas in C26a tumors, the tumor vasculature consists of smaller vessels [14].

Tumor Growth and Toxicity

Although the effects of carbogen breathing on tumor physiology and FU pharmacokinetics are stronger in C38 tumors than in C26a tumors, the direction of changes in both tumor lines favors an increased efficacy of FU when combined with carbogen breathing. The fact that C26a tumors profit more from carbogen breathing than do C38 tumors could be explained by their different tumor microenvironment. At the same tumor size, C26a tumors are less well vascularized than C38 tumors [14]. Previously, it has been shown by McSheehy et al. [9] that larger, presumably less-vascularized RIF-1 tumors profit more from carbogen breathing in terms of cytotoxic treatment efficacy than smaller, better-vascularized tumors.

It should be noted that, at the dose of FU used in the MRS experiments (150 mg/kg), enhanced toxicity and early deaths were observed in the group that underwent carbogen breathing. This is the first report of carbogen-induced toxicity, in combination with FU therapy. In patients, cardiac toxicity has been observed after continuous high-dose infusion of FU [35], and megakaryocytosis is a well-described effect of FU on the bone marrow [36]. Thus, pathological anatomic observations in this experiment (ischemic necrosis of the heart muscles, cardiac failure, and thrombocytosis) may be related to FU-induced systemic toxicity, and high levels of catabolites have been associated with cardiotoxicity [37–39]. In this study, no increase in catabolite levels in the group of mice that underwent carbogen breathing was observed. However, because catabolites are mainly produced in the liver and are taken up in the tumor through the blood circulation [40–43], the level of catabolites in the tumor is not necessarily correlated with catabolite levels in other organs, such as heart muscles.

In previous studies, no toxicity has been described after the combination of FU treatment with carbogen breathing. In fact, Griffiths et al. [44] showed that there were no significant effects of carbogen breathing on the levels of FU and its metabolites in normal rat tissues, and on the histology of tissues. In that study, FU was administered at a dose of 50 mg/kg, and carbogen was applied for a shorter time (10 minutes). Not only the administered dose of FU but also the duration of carbogen breathing may be crucial for the occurrence of systemic toxicity. In a recent study, increased clearance of FU from the plasma was observed after 30 minutes of carbogen breathing compared to 20 minutes of carbogen breathing [10]. If this increased clearance of FU

is caused by an increased uptake of FU in vital organs such as the heart muscles, this may well explain the observed toxicity.

In conclusion, these results show that, even within one tumor type, namely, colon carcinoma, the effects of carbogen breathing on tumor physiology and FU uptake and metabolism differ, which may be caused by differences in tumor vasculature. For clinical applications, this underscores the importance of an early analysis of response to carbogen breathing (e.g., by ^{19}F MRS) in individual patients. In the murine models C38 and C26a, an increase in FU uptake in the tumors was observed after carbogen breathing and FU efficacy in C26a tumors had increased. Because systemic toxicity was also enhanced, a clinical study evaluating the effect of carbogen breathing on FU efficacy should be preceded by a phase I trial monitoring the effect of carbogen breathing on FU toxicity.

Acknowledgements

The authors thank H. van Rennes for laboratory support; B. A. Lemmers-van de Weem, I. M. Lamers-Elmants, G. J. Grutters, M. Brom, and colleagues at the Central Animal Laboratory for biotechnical assistance and animal care; and G. Muda from the Department of Radiology for assistance with the ^{31}P and ^{19}F MRS measurements. The assistance of W. J. Peeters with the preparation of paraffin materials is kindly acknowledged.

References

- Van Laarhoven HW and Punt CJ (2004). Systemic treatment of advanced colorectal carcinoma. *Eur J Gastroenterol Hepatol* **16**, 283–289.
- Semenza GL (2000). Expression of hypoxia-inducible factor 1: mechanisms and consequences. *Biochem Pharmacol* **59**, 47–53.
- Gatenby RA and Gillies RJ (2004). Why do cancers have high aerobic glycolysis? *Nat Rev Cancer* **4**, 891–899.
- Teicher BA (1994). Hypoxia and drug resistance. *Cancer Metastasis Rev* **13**, 139–168.
- Van Laarhoven HW, Kaanders JH, Lok J, Peeters WJ, Rijken PF, Wiering B, Ruers TJ, Punt CJ, Heerschap A, and van der Kogel AJ (2006). Hypoxia in relation to vasculature and proliferation in liver metastases in patients with colorectal cancer. *Int J Radiat Oncol Biol Phys* **64**, 473–482.
- Rodrigues LM, Maxwell RJ, McSheehy PM, Pinkerton CR, Robinson SP, Stubbs M, and Griffiths JR (1997). *In vivo* detection of ifosfamide by ^{31}P -MRS in rat tumours: increased uptake and cytotoxicity induced by carbogen breathing in GH3 prolactinomas. *Br J Cancer* **75**, 62–68.
- Rodrigues LM, Robinson SP, McSheehy PM, Stubbs M, and Griffiths JR (2002). Enhanced uptake of ifosfamide into GH3 prolactinomas with hypercapnic hyperoxic gases monitored *in vivo* by $(31)\text{P}$ MRS. *Neoplasia* **4**, 539–543.
- Kamm YJ, Heerschap A, and Wagener DJ (2000). Effect of carbogen breathing on the pharmacodynamics of 5-fluorouracil in a murine colon carcinoma. *Eur J Cancer* **36**, 1180–1186.
- McSheehy PM, Robinson SP, Ojugo AS, Aboagye EO, Cannell MB, Leach MO, Judson IR, and Griffiths JR (1998). Carbogen breathing increases 5-fluorouracil uptake and cytotoxicity in hypoxic murine RIF-1 tumors: a magnetic resonance study *in vivo*. *Cancer Res* **58**, 1185–1194.
- McSheehy PM, Port RE, Rodrigues LM, Robinson SP, Stubbs M, van der Borns K, Peters GJ, Judson IR, Leach MO, and Griffiths JR (2005). Investigations *in vivo* of the effects of carbogen breathing on 5-fluorouracil pharmacokinetics and physiology of solid rodent tumours. *Cancer Chemother Pharmacol* **55**, 117–128.
- van der Sanden BP, Heerschap A, Hoofd L, Simonetti AW, Nicolay K, van der TA, Colier WN, and van der Kogel AJ (1999). Effect of carbogen breathing on the physiological profile of human glioma xenografts. *Magn Reson Med* **42**, 490–499.
- Al Hallaq HA, River JN, Zamora M, Oikawa H, and Karczmar GS (1998). Correlation of magnetic resonance and oxygen microelectrode measurements of carbogen-induced changes in tumor oxygenation. *Int J Radiat Oncol Biol Phys* **41**, 151–159.
- Van Laar JAM, Rustum YM, Van der Wilt CL, Smid K, Kuiper CM, Pinedo HM, and Peters GJ (1996). Tumor size and origin determine the antitumor activity of cisplatin or 5-fluorouracil and its modulation by leucovorin in murine colon carcinomas. *Cancer Chemother Pharmacol* **39**, 79–89.
- Van Laarhoven HW, Bussink J, Lok J, Punt CJ, Heerschap A, and van der Kogel AJ (2004). Effects of nicotinamide and carbogen in different murine colon carcinomas: immunohistochemical analysis of vascular architecture and microenvironmental parameters. *Int J Radiat Oncol Biol Phys* **60**, 310–321.
- Guerquin-Kern JL, Leteurre F, Croisy A, and Lhoste JM (1991). pH dependence of 5-fluorouracil uptake observed by *in vivo* ^{31}P and ^{19}F nuclear magnetic resonance spectroscopy. *Cancer Res* **51**, 5770–5773.
- Van Laarhoven HW, Punt CJ, Kamm YJ, and Heerschap A (2005). Monitoring fluoropyrimidine metabolism in solid tumors with *in vivo* $(19)\text{F}$ magnetic resonance spectroscopy. *Crit Rev Oncol Hematol* **56**, 321–343.
- Gambarota G, Van Laarhoven HW, Philippens M, Peeters M, Rijken W, van der Kogel PF, Punt AJ, and Heerschap CJ (2005). Relative blood volume and blood hemodynamics assessment by USPIO-induced T1 changes in MRI of murine colon carcinoma. *Proc Int Soc Magn Reson Med* **13**, 2111.
- Muda G, Van Laarhoven HW, Klomp DW, Pikkemaat J, van Asten J, Kamm YJ, and Heerschap A (2001). Double tuned coil for interleaved $^{31}\text{P}/^{19}\text{F}$ MRS of mouse tumors at 7 Tesla. *Proc Int Soc Magn Reson Med* **9**, 1106.
- Ojugo AS, McSheehy PM, McIntyre DJ, McCoy C, Stubbs M, Leach MO, Judson IR, and Griffiths JR (1999). Measurement of the extracellular pH of solid tumours in mice by magnetic resonance spectroscopy: a comparison of exogenous $(19)\text{F}$ and $(31)\text{P}$ probes. *NMR Biomed* **12**, 495–504.
- Barbier EL, St Lawrence KS, Grillon E, Koretsky AP, and Decors M (2002). A model of blood–brain barrier permeability to water: accounting for blood inflow and longitudinal relaxation effects. *Magn Reson Med* **47**, 1100–1109.
- Robinson SP, Howe FA, Stubbs M, and Griffiths JR (2000). Effects of nicotinamide and carbogen on tumour oxygenation, blood flow, energetics and blood glucose levels. *Br J Cancer* **82**, 2007–2014.
- Bussink J, Kaanders JH, Rijken PF, Peters JP, Hodgkiss RJ, Marres HA, and van der Kogel AJ (1999). Vascular architecture and microenvironmental parameters in human squamous cell carcinoma xenografts: effects of carbogen and nicotinamide. *Radiother Oncol* **50**, 173–184.
- Lanzen JL, Braun RD, Ong AL, and Dewhirst MW (1998). Variability in blood flow and pO_2 in tumors in response to carbogen breathing. *Int J Radiat Oncol Biol Phys* **42**, 855–859.
- Powell ME, Hill SA, Saunders MI, Hoskin PJ, and Chaplin DJ (1996). Effect of carbogen breathing on tumour microregional blood flow in humans. *Radiother Oncol* **41**, 225–231.
- Stubbs M, Robinson SP, Rodrigues LM, Parkins CS, Collingridge DR, and Griffiths JR (1998). The effects of host carbogen (95% oxygen/5% carbon dioxide) breathing on metabolic characteristics of Morris hepatoma 9618a. *Br J Cancer* **78**, 1449–1456.
- Ojugo AS, McSheehy PM, Stubbs M, Alder G, Bashford CL, Maxwell RJ, Leach MO, Judson IR, and Griffiths JR (1998). Influence of pH on the uptake of 5-fluorouracil into isolated tumour cells. *Br J Cancer* **77**, 873–879.
- Lemaire LP, McSheehy PM, and Griffiths JR (1998). Pre-treatment energy status of primary rat tumours as the best predictor of response to 5-fluorouracil chemotherapy: a magnetic resonance spectroscopy study *in vivo*. *Cancer Chemother Pharmacol* **42**, 201–209.
- Sijens PE, Huang YM, Baldwin NJ, and Ng TC (1991). ^{19}F magnetic resonance spectroscopy studies of the metabolism of 5-fluorouracil in murine RIF-1 tumors and liver. *Cancer Res* **51**, 1384–1390.
- van der Sanden BP, Rijken PF, Heerschap A, Bernsen HJ, and van der Kogel AJ (1997). *In vivo* $(31)\text{P}$ magnetic resonance spectroscopy and morphometric analysis of the perfused vascular architecture of human glioma xenografts in nude mice. *Br J Cancer* **75**, 1432–1438.

- [30] Jirtle RL (1988). Chemical modification of tumour blood flow. *Int J Hypertherm* **4**, 355–371.
- [31] Neeman M, Dafni H, Bukhari O, Braun RD, and Dewhirst MW (2001). In vivo BOLD contrast MRI mapping of subcutaneous vascular function and maturation: validation by intravital microscopy. *Magn Reson Med* **45**, 887–898.
- [32] Dunn TJ, Braun RD, Rhemus WE, Rosner GL, Secomb TW, Tozer GM, Chaplin DJ, and Dewhirst MW (1999). The effects of hyperoxic and hypercarbic gases on tumour blood flow. *Br J Cancer* **80**, 117–126.
- [33] Robinson SP, Rijken PF, Howe FA, McSheehy PM, van der Sanden BP, Heerschap A, Stubbs M, van der Kogel AJ, and Griffiths JR (2003). Tumor vascular architecture and function evaluated by non-invasive susceptibility MRI methods and immunohistochemistry. *J Magn Reson Imaging* **17**, 445–454.
- [34] Harrison L and Blackwell K (2004). Hypoxia and anemia: factors in decreased sensitivity to radiation therapy and chemotherapy? *Oncologist* **9** (5), 31–40.
- [35] de Forni M, Malet-Martino MC, Jaillais P, Shubinski RE, Bachaud JM, Lemaire L, Canal P, Chevreau C, Carrie D, and Soulie P (1992). Cardiotoxicity of high-dose continuous infusion fluorouracil: a prospective clinical study. *J Clin Oncol* **10**, 1795–1801.
- [36] Radley JM and Scurfield G (1979). Effects of 5-fluorouracil on mouse bone marrow. *Br J Haematol* **43**, 341–351.
- [37] Koenig H and Patel A (1970). Biochemical basis for fluorouracil neurotoxicity. The role of Krebs cycle inhibition by fluoroacetate. *Arch Neurol* **23**, 155–160.
- [38] Rengelshausen J, Hull WE, Schwenger V, Goggelmann C, Walter-Sack I, and Bommer J (2002). Pharmacokinetics of 5-fluorouracil and its catabolites determined by ^{19}F nuclear magnetic resonance spectroscopy for a patient on chronic hemodialysis. *Am J Kidney Dis* **39**, E10.
- [39] Arellano M, Malet-Martino M, Martino R, and Gires P (1998). The anti-cancer drug 5-fluorouracil is metabolized by the isolated perfused rat liver and in rats into highly toxic fluoroacetate. *Br J Cancer* **77**, 79–86.
- [40] Lutz NW, Naser-Hijazi B, Koroma S, Berger MR, and Hull WE (2004). Fluoropyrimidine chemotherapy in a rat model: comparison of fluorouracil metabolite profiles determined by high-field ^{19}F -NMR spectroscopy of tissues ex vivo with therapy response and toxicity for locoregional vs systemic infusion protocols. *NMR Biomed* **17**, 101–131.
- [41] Prior MJ, Maxwell RJ, and Griffiths JR (1990). In vivo ^{19}F NMR spectroscopy of the antimetabolite 5-fluorouracil and its analogues. An assessment of drug metabolism. *Biochem Pharmacol* **39**, 857–863.
- [42] Naser-Hijazi B, Berger MR, Schmah D, Schlag P, and Hull WE (1991). Locoregional administration of 5-fluoro-2'-deoxyuridine (FdUrd) in Novikoff hepatoma in the rat: effects of dose and infusion time on tumor growth and on FdUrd metabolite levels in tumor tissue as determined by ^{19}F -NMR spectroscopy. *J Cancer Res Clin Oncol* **117**, 295–304.
- [43] McSheehy PM, Seymour MT, Ojugo AS, Rodrigues LM, Leach MO, Judson IR, and Griffiths JR (1997). A pharmacokinetic and pharmacodynamic study in vivo of human HT29 tumours using ^{19}F and ^{31}P magnetic resonance spectroscopy. *Eur J Cancer* **33**, 2418–2427.
- [44] Griffiths JR, McIntyre DJ, Howe FA, McSheehy PM, Ojugo ASE, Rodrigues LM, Wadsworth P, Price NM, Lofts F, Nicholson G, et al. (2001). Issues of normal tissue toxicity in patient and animal studies—effect of carbogen breathing in rats after 5-fluorouracil treatment. *Acta Oncol* **40**, 609–614.